한국소음진동공학회 1998년도 춘계학술대회논문집, pp. 407~412.

충격해석을 위한 새로운 불연속 시간적분법의 개발

0 조진연*, 김승조*

Development of a New Discontinuous Time Integration Method for Transient Analysis of Impact Phenomena

Jin Yeon Cho, Seung Jo Kim

ABSTRACT

In this work, a new time integration method is proposed using the generalized derivative concept to simulate the dynamic phenomena having sudden constraint occurring in dynamic contact/impact problems. By the adoption of the generalized derivative concept and jump assumption, discontinuity can be incorporated in time integration and as a result, the algorithm does not need any other special consideration of jumps in dynamic field variables due to sudden constraint, like dynamic contact-release conditions. To observe the characteristics of the proposed time integration method, the stability and convergence analyses are carried out. In numerical tests, several dynamic contact/impact problems are analyzed by straightforward application of the proposed time integration method with the exterior penalty method.

I. Introduction

To simulate the contact/impact problems, several studies have been carried out and it has been pointed out that the impenetrability condition alone in the contact area is not sufficient in the numerical simulations of dynamic contact/impact problems. For the purpose, Hughes et al.[1] devised the discrete dynamic contact/impact conditions for lumped mass case and enforced the conditions. Taylor and Papadopoulos[2] assumed that the velocities and accelerations on the contact points are independent of the displacements in Newmark time integration method and enforced the velocity and the acceleration compatibility. Lee[3] proposed iterative scheme for satisfying the velocity and the acceleration compatibility on the contact surface under the constant average acceleration method.[4] The sudden constraint for dynamic impenetration induces the jumps in dynamic field variables and this makes it difficult to satisfy the velocity and the acceleration compatibility between target and impactor under discrete time integration such as Newmark method. As a result, straightforward application of the impenetrability condition without any other treatment produces undesirable oscillations. This fact is somewhat different issue in solving the static contact problems.

In this work, a new discontinuous time integration method is presented to overcome this trouble arising in the numerical simulation of the dynamic contact/impact problems.

* Department of Aerospace Engineering
Seoul National University

II. Discontinuous Time Integration Method

1. Discrete Operator for Time Integration

In the development of time integration method, the concept of the generalized derivative in distribution theory[5] and jump assumption are considered together since the definition of generalized derivative can provide the meaning of derivative even for a discontinuous distribution like Dirac delta function.[5] The definition of generalized derivative of distribution is constructed through the integration-by-parts. By the procedure, the difficulty of differentiation of a distribution is transferred to the differentiation of a test function. Using the concept, generalized relations for displacement $\mathbf{u}(t)$ ~ velocity $\mathbf{v}(t)$ and velocity $\mathbf{v}(t)$ ~ acceleration $\mathbf{a}(t)$ are constructed by integration-by-parts formula and jump assumptions as shown below.

$$\int_{t_0}^{t_f} \mathbf{w}^T \mathbf{v} dt = -\int_{t_0}^{t_f} \dot{\mathbf{w}}^T \mathbf{u} dt + \mathbf{w}^T \mathbf{u}\Big|_{t_0}^{t_f} \quad \text{for all } \mathbf{w}(t)$$

$$\int_{t_0}^{t_f} \mathbf{w}^T \mathbf{a} dt = -\int_{t_0}^{t_f} \dot{\mathbf{w}}^T \mathbf{v} dt + \mathbf{w}^T \mathbf{v}\Big|_{t_0}^{t_f} \quad \text{for all } \mathbf{w}(t) \qquad (1)$$

$$\mathbf{u}(t_0) \neq \mathbf{u}(t_0^+),\ \mathbf{v}(t_0) \neq \mathbf{v}(t_0^+),\ \text{and } \mathbf{a}(t_0) \neq \mathbf{a}(t_0^+)$$

where the jump conditions at the initial time t_0 are assumed for the natural imposition of abrupt loading. Superscript (+) denotes the right limt of time t_0 as shown

in Fig. 1. The test function is denoted by **w**. In contrary with dynamic field variables (i.e. **u**, **v**, and **a**), test function **w** is assumed to be continuous at t_0 to enforce the effect of initial condition. As a result, the above relations incorporates the jump due to shock loading condition.

For the temporal approximation, time domain of investigation is restricted to $[t_n=t_0,\ t_{n+1}=t_f]$ and the linear Lagrange interpolation functions ψ_i are used for approximating displacement **u**, velocity **v**, acceleration **a**, and test function **w**. The approximation vectors defined on an interval $t_n < t \le t_{n+1} = t + \Delta t$ are written in the following forms.

$$\begin{aligned} &\mathbf{u}(t) = \psi_i(t)\mathbf{u}_n^i,\ \mathbf{v}(t) = \psi_i(t)\mathbf{v}_n^i \\ &\mathbf{a}(t) = \psi_i(t)\mathbf{a}_n^i,\ \mathbf{w}(t) = \psi_i(t)\mathbf{w}_n^i \quad (i=0,1) \end{aligned} \tag{2}$$

where the summation convention is used for i and $(\bullet)_n^0$ and $(\bullet)_n^1$ denote field values at time t_n^+ and t_{n+1}^-, respectively. They are shown in Fig. 1. For a higher order approximation, higher order interpolation functions can be used as in Kim et al.[6] By the substitution of interpolating functions (2) into equation (1), approximated relations for time derivative are obtained. The relations are written as follows through reordering.

For all $\mathbf{w}_n^i$ $(i=0,\ 1)$,

$$\begin{aligned} &\int_{t_n}^{t_{n+1}} \dot{\psi}_i\psi_j \mathbf{w}_n^{iT}\mathbf{u}_n^j dt - \mathbf{w}^T\mathbf{u}\Big|_{t_{n+1}} = -\int_{t_n}^{t_{n+1}} \psi_i\psi_j \mathbf{w}_n^{iT}\mathbf{v}_n^j dt - \mathbf{w}^T\mathbf{u}\Big|_{t_n} \\ &\int_{t_n}^{t_{n+1}} \dot{\psi}_i\psi_j \mathbf{w}_n^{iT}\mathbf{v}_n^j dt - \mathbf{w}^T\mathbf{v}\Big|_{t_{n+1}} = -\int_{t_n}^{t_{n+1}} \psi_i\psi_j \mathbf{w}_n^{iT}\mathbf{a}_n^j dt - \mathbf{w}^T\mathbf{v}\Big|_{t_n} \\ &\mathbf{u}(t_n) = \mathbf{u}_{n-1}^1,\ \mathbf{v}(t_n) = \mathbf{v}_{n-1}^1,\ \mathbf{a}(t_n) = \mathbf{a}_{n-1}^1,\ \ \mathbf{w}(t_n) = \mathbf{w}_n^0 \\ &\mathbf{u}(t_{n+1}) = \mathbf{u}_n^1,\ \mathbf{v}(t_{n+1}) = \mathbf{v}_n^1,\ \mathbf{a}(t_{n+1}) = \mathbf{a}_n^1,\ \ \mathbf{w}(t_{n+1}) = \mathbf{w}_n^1 \end{aligned} \tag{3}$$

where the summation convention notation is used.

In equation (3), the dynamic field variables **u**, **v**, and **a** contain the discontinuities at the initial time t_0 ($= t_n$). The $\mathbf{u}_{n-1}^1$, $\mathbf{v}_{n-1}^1$, and $\mathbf{a}_{n-1}^1$ are the given initial vector obtained from the previous time step. The effect of the initial condition is weakly imposed via $\mathbf{u}_{n-1}^1$, $\mathbf{v}_{n-1}^1$, and $\mathbf{a}_{n-1}^1$. Since equation (3) must hold for all $\mathbf{w}_n^i$, it can be written in simplified matrix form as

$$\begin{aligned} \hat{\Phi}\mathbf{U}_{n+1} &= \Phi\mathbf{V}_{n+1} + \Theta\mathbf{U}_n \\ \hat{\Phi}\mathbf{V}_{n+1} &= \Phi\mathbf{A}_{n+1} + \Theta\mathbf{V}_n \end{aligned} \tag{4}$$

where $\mathbf{U}_{n+1} = \left\{\mathbf{u}_n^{0T}, \mathbf{u}_n^{1T}\right\}^T$, $\mathbf{V}_{n+1} = \left\{\mathbf{v}_n^{0T}, \mathbf{v}_n^{1T}\right\}^T$, $\mathbf{A}_{n+1} = \left\{\mathbf{a}_n^{0T}, \mathbf{a}_n^{1T}\right\}^T$

The alternative forms for displacement-velocity and velocity-acceleration relations are obtained by the inversion.

$$\begin{aligned} \mathbf{U}_{n+1} &= \overline{\Psi}\mathbf{V}_{n+1} + \overline{\Psi}_0\mathbf{V}_n + \mathbf{J}\mathbf{U}_n \\ \mathbf{V}_{n+1} &= \overline{\Psi}\mathbf{A}_{n+1} + \overline{\Psi}_0\mathbf{A}_n + \mathbf{J}\mathbf{V}_n \end{aligned} \tag{5}$$

where $\overline{\Psi} = \hat{\Phi}^{-1}\Phi$, $\overline{\Psi}_0 = \mathbf{0}$, $\mathbf{J} = \hat{\Phi}^{-1}\Theta$. Using the discrete operators of equation (5), numerical time integration algorithm is constructed with the dynamic equilibrium equation.

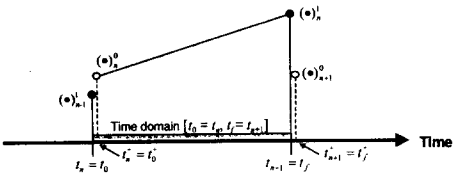

Fig. 1 Description of time domain and jumps of variables

2. Numerical Time Integration Algorithm

The dynamic equilibrium equation of a dynamic system discretized in space domain is given as follows.

$$\mathbf{m}\mathbf{a} + \mathbf{c}\mathbf{v} + \mathbf{k}\mathbf{u} = \mathbf{f} \tag{6}$$

where **m** , **c**, and **k** are mass, damping, and stiffness matrices, respectively. External force vector is denoted by **f**. With the discrete operator (5), the dynamic equilibrium equations at the inner time steps (i.e. t_n^+ and t_{n+1}^-) are used to obtain a time integration algorithm.

$$\mathbf{m}\mathbf{a}_n^i + \mathbf{c}\mathbf{v}_n^i + \mathbf{k}\mathbf{u}_n^i = \mathbf{f}_n^i, \quad (i=0,1) \tag{7}$$

Using the matrix notation, it can be denoted as

$$\mathbf{M}\mathbf{A}_{n+1} + \mathbf{C}\mathbf{V}_{n+1} + \mathbf{K}\mathbf{U}_{n+1} = \mathbf{F}_{n+1} \tag{8}$$

where **M**, **C**, and **K** are block diagonal matrices for mass, damping, and stiffness, respectively and **F** denotes the forcing vector. To obtain the dynamic field variables $\mathbf{A}_{n+1}$, $\mathbf{V}_{n+1}$, $\mathbf{U}_{n+1}$, it is sufficient to solve the equations (5) and (8), simultaneously. As a result, the numerical time integration algorithm is reduced to solving the following system of algebraic equations.

For the given initial conditions $\mathbf{A}_n, \mathbf{V}_n, \mathbf{U}_n$,

find $\mathbf{A}_{n+1}, \mathbf{V}_{n+1}, \mathbf{U}_{n+1}$ *of the next time step such that*

$$\begin{aligned} \mathbf{U}_{n+1} &= \overline{\Psi}\mathbf{V}_{n+1} + \overline{\Psi}_0\mathbf{V}_n + \mathbf{J}\mathbf{U}_n \\ \mathbf{V}_{n+1} &= \overline{\Psi}\mathbf{A}_{n+1} + \overline{\Psi}_0\mathbf{A}_n + \mathbf{J}\mathbf{V}_n \\ \mathbf{M}\mathbf{A}_{n+1} &+ \mathbf{C}\mathbf{V}_{n+1} + \mathbf{K}\mathbf{U}_{n+1} = \mathbf{F}_{n+1} \end{aligned} \tag{9}$$

The system of algebraic equations for time stepping numerical integration can be rewritten by predictor-corrector form. The detail algorithm construction procedure is similar as in the paper of Kim et al.[6] The predictor-corrector algorithm based on displacement form is as follows.

i) Calculate $\mathbf{a}_0$ *such that* $\mathbf{m}\mathbf{a}_0 + \mathbf{c}\mathbf{v}_0 + \mathbf{k}\mathbf{u}_0 = \mathbf{f}_0$

Set $\mathbf{A}_0 = \{\mathbf{0}^T, \mathbf{a}_0^T\}^T$, $\mathbf{V}_0 = \{\mathbf{0}^T, \mathbf{v}_0^T\}^T$, $\mathbf{U}_0 = \{\mathbf{0}^T, \mathbf{u}_0^T\}^T$

ii) Calculate $\mathbf{K}^{eff} = \mathbf{M}\overline{\Psi}^{-2} + \mathbf{C}\overline{\Psi}^{-1} + \mathbf{K}$ *and* $\mathbf{K}^{eff^{-1}}$

iii) Do n=0

$$\textit{Predict} \begin{cases} \tilde{\mathbf{A}}_{n+1}^{(u)} = -\overline{\Psi}^{-1}\overline{\Psi}_0\mathbf{A}_n - \overline{\Psi}^{-2}\mathbf{J}\mathbf{U}_n \\ \qquad\qquad -(\overline{\Psi}^{-2}\overline{\Psi}_0 + \overline{\Psi}^{-1}\mathbf{J})\mathbf{V}_n \\ \tilde{\mathbf{V}}_{n+1}^{(u)} = -\overline{\Psi}^{-1}\overline{\Psi}_0\mathbf{V}_n - \overline{\Psi}^{-1}\mathbf{J}\mathbf{U}_n \end{cases} \tag{10}$$

$$\textit{Calculate} \begin{cases} \mathbf{R}_{n+1}^{(u)} = \mathbf{F}_{n+1} - \mathbf{M}\tilde{\mathbf{A}}_{n+1}^{(u)} - \mathbf{C}\tilde{\mathbf{V}}_{n+1}^{(u)} \\ \mathbf{U}_{n+1} = \mathbf{K}^{eff^{-1}}\mathbf{R}_{n+1}^{(u)} \end{cases} \tag{11}$$

$$\textit{Correct} \quad \begin{cases} \mathbf{A}_{n+1} = \tilde{\mathbf{A}}^{(u)}_{n+1} + \overline{\Psi}^{-2}\mathbf{U}_{n+1} \\ \mathbf{V}_{n+1} = \tilde{\mathbf{V}}^{(u)}_{n+1} + \overline{\Psi}^{-2}\mathbf{U}_{n+1} \end{cases} \tag{12}$$

Set $n = n+1$

Continue

where $\tilde{\mathbf{A}}^{(u)}_{n+1}$ and $\tilde{\mathbf{V}}^{(u)}_{n+1}$ have the meaning of predictors for acceleration and velocity, respectively. After the initialization and predictor stage, the displacements are obtained via equation (11). The acceleration and velocity are corrected by the correction equation (12).

3. Stability and Accuracy Analysis

To guarantee the unconditional stability of a time integration algorithm[6], all the magnitudes of amplification factors of the algorithm (i.e. magnitude of eigenvalue) must be less than or equal to 1. The Fig. 2 shows the magnitude of amplification factor(spectral radius). From Fig. 2, it is shown that the proposed method is unconditionally stable because all the magnitudes of amplification factors are less than or equal to 1. Moreover, the method decays out the high frequency responses compared to time step Δt (i.e. $\Delta t/T > 1$) since the amplification factor is zero in that region. The property gives filtering effect of high frequency noise.

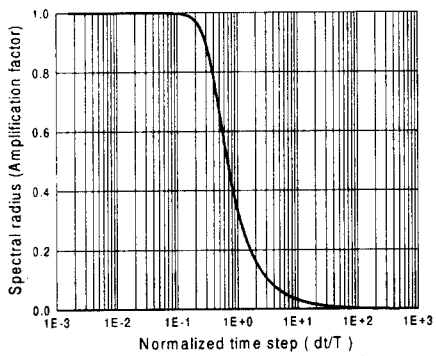

Fig. 2 Spectral radius vs. normalized time step

To observe the accuracy of the proposed time integration method, the free-oscillation problem with unit mass and stiffness is solved and the amplitude decay error and period elongation error[4,7] are shown in Fig. 3. The slope of curve is the order of convergence. The results show that the proposed method has the third-order convergence in amplitude and the fourth-order convergence in period. Thus it can be concluded that the proposed method (linear approximation in time) has the third-order convergence at least in combined cases and is more accurate than the Newmark constant average acceleration method which has the second-order convergence.[6] In Fig. 4, the time domain response of free-oscillation system is given and compared with exact solution and the result obtained by the constant average acceleration. It crearly shows that the proposed method is much more accurate than the Newmark constant average acceleration method.

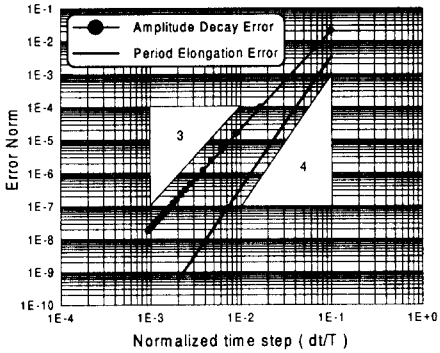

Fig. 3 Log-scale plot of error norm vs. normalized time step

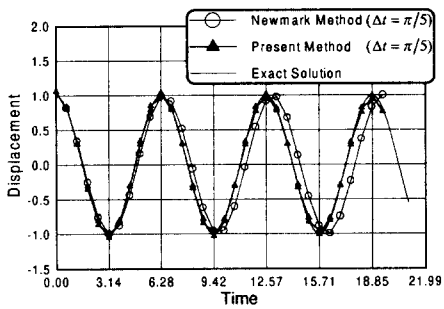

Fig. 4 Comparison of time domain responses of free-oscillation problem

III. Dynamic Contact/Impact Problems

1. Variational Formulation of Impact Problems

Consider an elastic body Ω with a boundary Γ impacted by a rigid body R in two-dimensional space. Then the dynamic process of system is described by the governing equations for each body. The impenetrability condition[8] on the contact surface can be written by the inequality equation.

$$\boldsymbol{u}\cdot\boldsymbol{n} \le s(\boldsymbol{x},\boldsymbol{q},\theta) \text{ on } \Gamma_C \tag{13}$$

where $\boldsymbol{n}$ is outward unit normal vector on Γ_C and s denotes contact gap. Coordinate, displacement of target, displacement of impactor and rotation of impactor are denoted by $\boldsymbol{x}$, $\boldsymbol{u}$, $\boldsymbol{q}$, and θ. In contact boundary the normal traction component is negative if there is contact. The tangential traction vector on contact boundary is zero with the assumption of no friction. The variational form is derived from the principle of virtual work. In the variational formulation, both the rigid impactor and solid target are incorporated and penalized external virtual work from the exterior penalty method[8] is added in order to satisfy the contact condition. Then the equilibrium equation can be written as the following variational form.

$$\left\{\begin{array}{l}\int_\Omega \rho\,\ddot{\boldsymbol{u}}\cdot\delta\boldsymbol{u}\,d\Omega+\int_\Omega \boldsymbol{\sigma}\cdot\delta\boldsymbol{\varepsilon}\,d\Omega \\ -\int_\Omega \boldsymbol{f}\cdot\delta\boldsymbol{u}\,d\Omega-\int_{\Gamma_F}\bar{\boldsymbol{t}}\cdot\delta\boldsymbol{u}\,dS \\ +(m_R\,\ddot{\boldsymbol{q}}-\boldsymbol{f}_R)\cdot\delta\boldsymbol{q}+(I_R\ddot{\theta}-N_R)\cdot\delta\theta \\ +\dfrac{1}{\varepsilon_p}\left[\begin{array}{l}\int_{\Gamma_C}(\boldsymbol{u}\cdot\boldsymbol{n}-s)^+\boldsymbol{n}\cdot\delta\boldsymbol{u}\,dS \\ -\int_{\Gamma_C}(\boldsymbol{u}\cdot\boldsymbol{n}-s)^+\dfrac{ds}{d\boldsymbol{q}}\cdot\delta\boldsymbol{q}\,dS \\ -\int_{\Gamma_C}(\boldsymbol{u}\cdot\boldsymbol{n}-s)^+\dfrac{ds}{d\theta}\cdot\delta\theta dS\end{array}\right]\end{array}\right\}=0 \qquad (14)$$

where ρ is density, $\boldsymbol{\sigma}$ is stress, and $\boldsymbol{t}$ is traction. Subscripts D and F denote displacement and force boundary, respectively. m_R, $\boldsymbol{f}_R$, I_R, and N_R denote mass, applied force, moment of inertia, and applied moment of the impactor, respectively. $\psi^+(\mathbf{x})=\boldsymbol{max}\{\psi(\mathbf{x}),0\}$ is a non-differentiable function and ε_p is a penalty parameter. The penalty terms in equation (14) make the problem nonlinear. The normal traction component on the contact boundary can be obtained by

$$\boldsymbol{n}\cdot\boldsymbol{\sigma}\cdot\boldsymbol{n}=-\frac{1}{\varepsilon_p}(\boldsymbol{u}\cdot\boldsymbol{n}-s)^+ \qquad (15)$$

2. Finite Element Approximation and Application of Time Integration

For the finite element approximation, the coordinate $\boldsymbol{x}$, displacement $\boldsymbol{u}$, and the strain $\boldsymbol{\varepsilon}$ in an element are interpolated by n-node isoparametric plane strain element.

$$\boldsymbol{x}=\sum_{i=1}^{n}\phi_i\mathbf{x}_i=\boldsymbol{H}\boldsymbol{x}_e,\ \boldsymbol{u}=\sum_{i=1}^{n}\phi_i\,\boldsymbol{u}_i=\boldsymbol{H}\boldsymbol{u}_e,\ \boldsymbol{\varepsilon}=\sum_{i=1}^{n}\boldsymbol{B}_i\boldsymbol{u}_i=\boldsymbol{B}\boldsymbol{u}_e \qquad (16)$$

Using equations (14) and (16), the discretized equation can be obtained by assembling the element matrices and the equation of rigid impactor.

$$\mathbf{m}\ddot{\mathbf{u}}+(\mathbf{k}+\frac{1}{\varepsilon_p}\mathbf{k}_N(\mathbf{u}))\mathbf{u}=\mathbf{f}+\frac{1}{\varepsilon_p}\mathbf{f}_N(\mathbf{u}) \qquad (17)$$

where roman face $\mathbf{u}$ denotes global displacement vector and $\mathbf{m}$, $\mathbf{k}$, $\mathbf{f}$ mean global mass, stiffness matrices and force vector, respectively. The trapezoidal rule[8] is used instead of the Gauss quadrature rule in numerical integration of $\mathbf{k}_N$ and $\mathbf{f}_N$. To obtain the time dependent behavior of the dynamic system, the discretized governing equation (17) is integrated directly by the developed time integration method in the previous section without additional constraint like contact-release condition or special modification. The equilibrium equations at the inner time step (i) of time interval $[t_n, t_{n+1}]$ are written as shown below.

$$\mathbf{m}\mathbf{a}_n^i+(\mathbf{k}+\frac{1}{\varepsilon_p}\mathbf{k}_N(\mathbf{u}_n^i))\mathbf{u}_n^i=\mathbf{f}_n^i+\frac{1}{\varepsilon_p}\mathbf{f}_N(\mathbf{u}_n^i),i=0,1 \qquad (18)$$

By matrix form, it is rewritten by using the notation in previous section.

$$\mathbf{M}\mathbf{A}_{n+1}+(\mathbf{K}+\mathbf{K}_N(\mathbf{U}_{n+1}))\mathbf{U}_{n+1}=\mathbf{F}_{n+1}+\mathbf{F}_N(\mathbf{U}_{n+1}) \qquad (19)$$

For the time integration, it is suffice to solve the system of equations (5) and (19). As a result, direct application of the proposed time integration method to the equation (19) yields the following fully discretized dynamic equilibrium equation.

$$(\hat{\mathbf{K}}+\mathbf{K}_N(\mathbf{U}_{n+1}))\mathbf{U}_{n+1}=\hat{\mathbf{F}}_{n+1}+\mathbf{F}_N(\mathbf{U}_{n+1}) \qquad (20)$$

where $\hat{\mathbf{K}}=\mathbf{M}\overline{\Psi}^{-2}+\mathbf{K}$ and

$\hat{\mathbf{F}}_{n+1}=\mathbf{F}_{n+1}+\mathbf{M}(\overline{\Psi}^{-1}\overline{\Psi}_0\mathbf{A}_n+(\overline{\Psi}^{-2}\overline{\Psi}_0+\overline{\Psi}^{-1}\mathbf{J})\mathbf{V}_n+\overline{\Psi}^{-2}\mathbf{J}\mathbf{U}_n)$

To solve the system of nonlinear algebraic equations, the successive iteration scheme[8] is used. Application of the successive iteration scheme yields the system of equations for iteration as follows.

$$(\hat{\mathbf{K}}+\mathbf{K}_N(\mathbf{U}_{n+1}^{(k-1)}))\mathbf{U}_{n+1}^{(k)}=\hat{\mathbf{F}}_{n+1}+\mathbf{F}_N(\mathbf{U}_{n+1}^{(k-1)}) \qquad (21)$$

where k denotes iteration number in each time step. Relative error of displacement is used as convergence criterion. Iteration is carried out until the relative error is less than the given tolerance 10^{-6}.

IV. Numerical Simulations

By the developed computer code based on the fully discretized equation (21), several dynamic contact/impact problems are computed. In the numerical simulations, the examples are compared with the results of Newmark constant acceleration method to show the accuracy and stability of the proposed algorithm.

1. Bar Impact

To check the validity of the developed code for analyzing the dynamic contact/impact problem, the typical bar impact problem in Fig. 5 is analyzed.

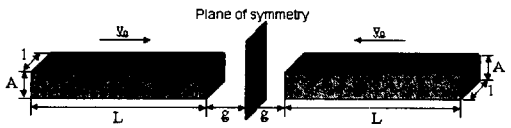

Fig. 5 Impact of two identical bars

The results are compared with the analytic solution. Two hundred plane strain elements (4 node isoparametric element) are used and time step size is 1 μsec. Since the problem has symmetric nature, one side of impact bar is discretized. The material properties and the dimensions for the problem are as follows : E = 100 GPa, A=2 cm, g=0 cm, ρ=1000 kg/m^3, L=30 cm, v_0=10 m/sec, where E is Young's modulus, A is thickness(cross section area per unit length), g is initial gap, L is length, and v_0 is the initial velocity of bar. In simulation of bar impact, Poisson's ratio ν is set to be 0. The contact force obtained by analytical method is 2×10^6 N at 0 μsec≤ t ≤ 60 μsec and zero at t > 60 μsec.

The contact force histories shown in Fig. 6 are the results of computation by the direct application of

Newmark constant average acceleration method for several penalty parameters.

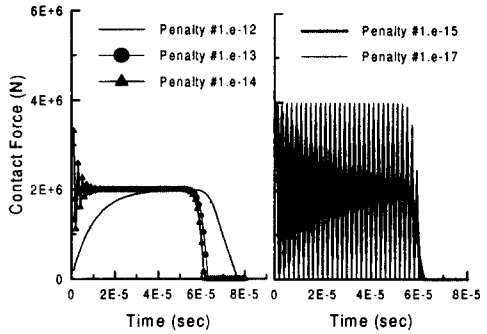

Fig. 6 Contact force history of bar impact using Newmark constant average acceleration method

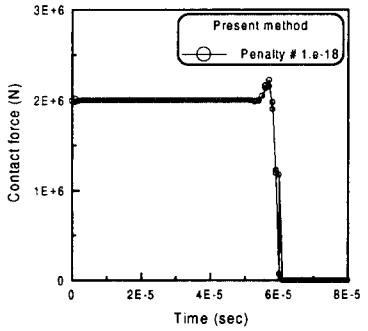

Fig. 7 Contact force history of bar impact using the present time integration method.

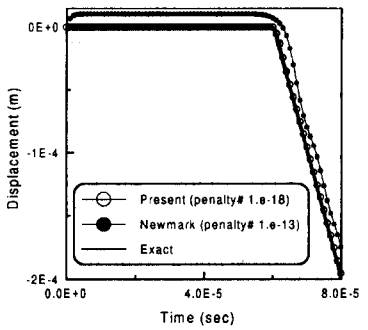

Fig. 8 Displacement history of contact node (bar impact)

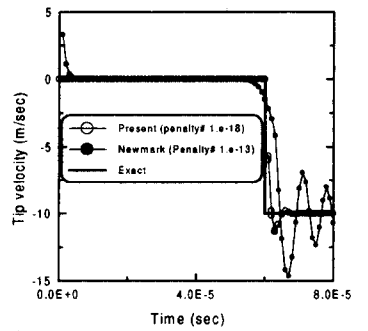

Fig. 9 Velocity history of contact node (bar impact)

From the results, it is observed that the direct use of Newmark constant average acceleration method without additional constraint like contact-release condition produces undesirable oscillation.[3] It is also observed that the oscillation increases as the penalty parameter is decreased.[9]

However, the direct use of proposed method gives stable solution in spite of smaller penalty parameter of 1.e-18 as shown in Fig. 7. In Fig. 8 and 9, the displacement and the velocity of contact node are plotted. For the Newmark case, the results of penalty parameter of 1.e-13 are presented, since the contact force of that is not oscillatory. The result in Fig. 8 shows that penetration occurs in Newmark case, however, the proposed method does not allow the penetration. It is observed in Fig. 9 that the proposed method successfully describes the velocity jump at time t=0. From the results, it can be verified that the proposed method is adequate in dynamic contact/ impact problems.

2. Impact of Isotropic Solid with Rigid Cylinder

As the second example, the impact behavior of solid block with rigid cylinder is simulated by both of the Newmark constant average acceleration method and the proposed method. The material properties and the dimensions for the model problem are as follows : ρ=2710kg/m^3, E=70Gpa, ν=0.3, L=3cm, A=1cm, m=65.8g, v_0=10m/sec, R=1 cm, where m is the mass of impactor, v_0 is the initial velocity of impactor, and R is the radius of impactor. Total number of nodes in finite element model is 1681 and element number is 1600. For the time integration, 0.2 μsec of time step size is used. Bottom is fixed in y-direction and both sides are fixed in x-direction. In simulation, symmetric condition is utilized. The finite element model used in the analysis is shown in Fig. 10.

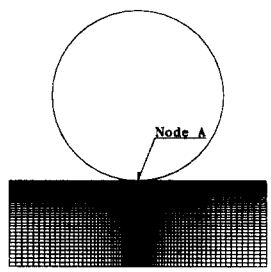

Fig. 10 Finite Element Model

Fig. 11 shows contact force history. It is observed that the results by Newmark method show numerical instability in penalty parameter of 1.e-16, whereas the proposed method gives stable solution in smaller penalty parameter of 1.e-18.

Displacement and velocity of rigid cylinder(impactor) and contact node(target) are shown in Fig. 12 and 13, respectively. Direct application of Newmark method allows penetration in penalty parameter of 1.e-15 which gives feasible contact force. Moreover it produces undesirable oscillation in velocity field. However, the impenetrability condition and velocity compatibility at contact region are precisely satisfied by the proposed

method. Especially, if the proposed method is used, the velocity jump at the outset of impact is numerically realized due to the intrinsic formulation containing the jump discontinuity.

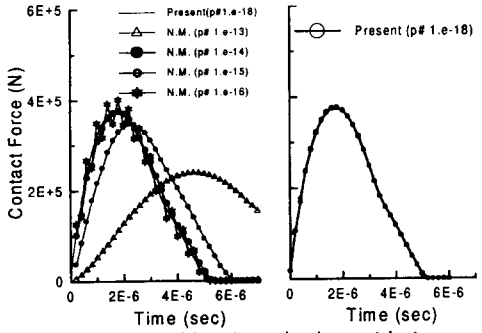

Fig. 11 Contact force history under impact between solid block and rigid cylinder

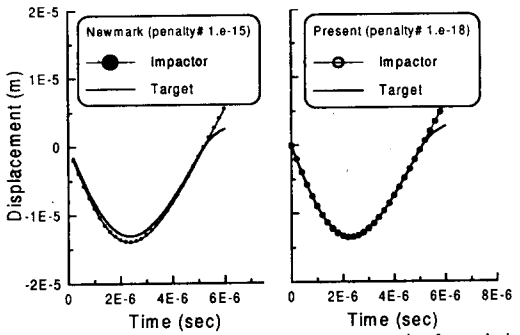

Fig. 12 Displacement history of contact node A and rigid cylinder

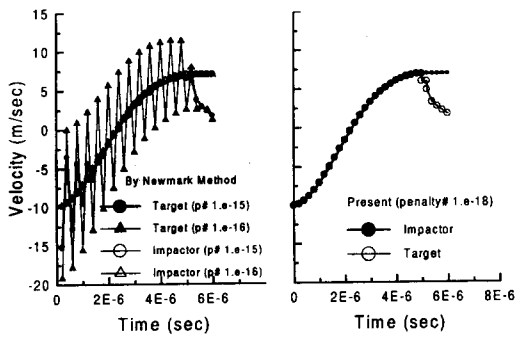

Fig. 13 Velocity history of contact node A and rigid cylinder

V. Concluding Remarks

A new time integration algorithm for the dynamic phenomena having sudden constraint occurring in dynamic contact/impact analysis is developed using the concept of generalized derivative. Using the generalized derivative concept and jump assumption, the jump discontinuity can be naturally incorporated in numerical time integration.

To observe the characteristics of the proposed time integration method, the stability and convergence analyses are carried out. The analyses proves that the proposed method gives unconditional stability and the third order accuracy at least. In numerical examples, several dynamic contact/impact problems are analyzed by straightforward application of the proposed time integration method with the exterior penalty method. The simulation results are compared with the results of computation by the Newmark constant average acceleration method. From the tests, it has been verified that the proposed time integration method can be used successfully in the numerical simulations of dynamic contact/impact phenomena.

Acknowledgement

The Authors would like to acknowledge the partial financial support from SERI Supercomputer Center through CRAY R&D Grant Program.

References

[1] Hughes, T.J.R., Taylor, R.L., Sackman, J. L., Curnier, A., and Kanoknukulchai, W., "A Finite Element Method for a Class of Contact-Impact Problems", *Computer Method in Applied Mechanics and Engineering*, Vol. 8, 1976, pp.249-276

[2] Taylor, R. L. and Papadopoulos, P., "On a Finite Element Method for Dynamic Contact/Impact Problems", *International Journal for Numerical Methods in Engineering*, Vol. 36, 1993, pp. 2123-2140

[3] Lee, K., "A Numerical solution for Dynamic Contact Problems satisfying the Velocity and Acceleration Compatibilities on the Contact Surface", *Computational Mechanics*, Vol. 15, 1994, pp. 189-200

[4] Bathe, K. J., *Finite Element Procedures*, International Ed., Prentice-Hall, Englewood Cliffs, NJ, 1996, Chap. 9.

[5] Reddy, B. D., *Functional Analysis and Boundary-Value Problems: an Introductory Treatment*, John Wiley and Sons, New York, 1986

[6] Kim, S. J., Cho, J. Y., and Kim, W. D., "From the Trapezoidal rule to Higher Order Accurate and Unconditionally Stable Time Integration Method for Structural Dynamics," *Computer Method in Applied Mechanics and Engineering*, Vol.149, 1997, pp. 73-88.

[7] Kim, S. J., and Cho, J. Y., " Penalized Weighted Residual Method for the Initial Value Problems," *AIAA Journal*, Vol. 35, No.1, 1997, pp.172-177

[8] Oden, J. T., and Carey, G. G., *Finite Element, Vol. V, Special Problems in Solid Mechanics*, Prentice-Hall, Englewood Cliffs, NJ, 1984, Chap. 4.

[9] Zhong, Z. H., *Finite element Procedures for Contact-Impact Problems*, Oxford University Press, New York, 1993, Chap. 4.